

JAERI - M  
87-013

INVESTIGATION OF A Nb-Ti CABLE-IN-CONDUIT  
CONDUCTOR:  
EXPERIMENTAL RESULTS

February 1987

P. E. PHELAN\*

JAERI-M レポートは、日本原子力研究所が不定期に公刊している研究報告書です。

入手の問い合わせは、日本原子力研究所技術情報部情報資料課（〒319-11 茨城県那珂郡東海村）  
あて、お申しこしてください。なお、このほかに財団法人原子力弘済会資料センター（〒319-11 茨城  
県那珂郡東海村日本原子力研究所内）で複写による実費頒布をおこなっております。

JAERI-M reports are issued irregularly.

Inquiries about availability of the reports should be addressed to Information Division, Department  
of Technical Information, Japan Atomic Energy Research Institute, Tokai-mura, Naka-gun,  
Ibaraki-ken 319-11, Japan.

© Japan Atomic Energy Research Institute, 1987

---

編集兼発行 日本原子力研究所  
印刷 山田軽印刷所

Investigation of a Nb-Ti Cable-in-Conduit Conductor :  
Experimental Results

P.E. PHELAN\*

Department of Thermonuclear Fusion Research  
Naka Fusion Research Establishment  
Japan Atomic Energy Research Institute  
Naka-machi, Naka-gun, Ibaraki-ken

(Received January 26, 1987)

A NbTi, Cable-in-conduit sample coil was experimentally investigated by using inductive heat inputs of durations 0.44 and 2.1 msec. Since the original goal of determining the effect of varying conductor perimeter on stability could not be achieved, the stability parameters which were studied and reported include mass flow rate, heating duration, and the presence of liquid helium outside of the conduit versus a surrounding vacuum. In addition, quench-induced pressure rises, both at zero and non-zero imposed flow rates, were measured. Results indicate that stability increases with imposed mass flow, stability increases with heating duration before the limiting current, and helium outside of the conduit has no discernible effect on transient stability. A detailed analysis of these findings will be published in the future.

Keywords : Cable-in-conduit, Force-cooled, Stability,  
Mass Flow Rate, Heating Duration, Superconducting

---

\* visiting student from the Massachusetts Institute of Technology

ケーブル・イン・コンジット型 Nb-Ti 超電導  
導体特性の実験的研究結果

日本原子力研究所那珂研究所核融合研究部

P. E. Phelan\*

(1987年1月26日受理)

ケーブル・イン・コンジット型の Nb-Ti 超電導導体の特性について、加熱時間 0.44 ms 及び 2.1 ms の誘導加熱を用いて測定を行なった。当初の研究課題であった導体冷却周長と導体安定性の関係については未完となったがヘリウムの流量、誘導加熱時間及び導体周辺の液体ヘリウムの有無等に対する導体安定性の依存性が測定された。又、ヘリウム強制流の有無に対するフェンチ時最大圧力の相違についても実験的な比較を行なった。

本実験結果から得られた主な結論としては、ヘリウムを強制的に流すことによって導体の安定性が顕著に増大すること、制限電流値以下では安定性マージンが加熱時間とともに増大すること、導体周辺の液体ヘリウムは、導体の過渡的安定性に寄与しないことが示された。

Contents

|   |    |
|---|----|
| 1. Introduction .....                           | 1  |
| 2. Experimental Parameters and Facilities ..... | 3  |
| 3. Experimental Procedure .....                 | 14 |
| 4. Results .....                                | 18 |
| 5. Conclusions and Recommendations .....        | 26 |
| Appendix .....                                  | 27 |
| References .....                                | 33 |
| Acknowledgments .....                           | 35 |

目 次

|                      |    |
|----------------------|----|
| 1. はじめに .....        | 1  |
| 2. 実験装置及びパラメータ ..... | 3  |
| 3. 実験方法 .....        | 14 |
| 4. 実験結果 .....        | 18 |
| 5. 結論及び今後への示唆 .....  | 26 |
| 6. 補 遺 .....         | 27 |
| 参 考 文 献 .....        | 33 |
| 謝 辞 .....            | 35 |

## 1. Introduction

Superconducting magnets have been with us since 1911 when Onnes discovered the existence of superconductivity. At that time, however, no practical use could be made of these magnets due to the relatively low critical fields and currents of the early conductors. It took the advent of superconducting alloys, such as the currently popular niobium titanium and niobium tin alloys, to make possible some realization of the potential of such magnets. Examples of applications, both for the present and for the future, include tools for high energy physics research, such as bubble chambers and particle accelerators, dc motors, magnetically-levitated trains, magnetohydrodynamic power generation, energy storage, and, most importantly with regard to this work, power generation from magnetically-confined controlled thermonuclear fusion. Indeed, it is this last area which has been the object of much recent international collaboration. [1]

Concentrated effort is required in several areas of superconducting research in order to realize a practical fusion reactor. These include (in no particular order): (1) improving the superconducting material itself so as to increase the critical field, the critical temperature, and the critical current density; (2) raising the strength of structural materials at liquid helium temperatures so that less space is required for structural support, thereby devoting more space to the conductor; (3) improving refrigeration and general cryogenic techniques so that less power has to be expended in this manner and, perhaps more importantly, making the entire cryogenic system more reliable; (4) investigating the use of different cryogenic fluids, namely helium II, which would allow for operating temperatures even lower than those in atmospheric pressure and supercritical helium; and (5) increasing the stability of the magnet against heat inputs, which include relatively long, low-power disturbances from neutron irradiation and short, relatively high-power disturbances arising from the motion of the conductor and also from eddy currents generated during pulsed operation of the coil. The power and time scale of the thermal input from "nuclear heating" is perhaps less than 50 mJ per cubic centimeter of conductor for one minute, whereas that of the shorter disturbances is maybe 300 mJ/cc for one millisecond. [2],[3] It is the topic of superconductor stability, especially against the shorter, high-power thermal inputs, with which this paper is principally concerned.

Two general types of superconductors can be found today. One is the older, "pool-boiling cooled" type (PBC) and the other is the "forced-flow cooled" type (FFC). This paper is an investigation of the latter's stability characteristics. The principal advantages offered by an FFC conductor as opposed to a PBC conductor are 1) better insulation; 2) greater rigidity against electromagnetic forces; and 3) lower pulsed loss due to the relatively smaller diameter conducting strands which can be used since less mechanical strength is required of the strands.

The principal disadvantages are 1) the pumping power required for their operation, which has to be dissipated at cryogenic temperatures; 2) the long time required for a "hot zone" to be transported away from the conductor; and 3) the limitation on the heat capacity available for cooling brought about by the small helium inventory. An example of where an FFC conductor would perhaps be more suitable than a PBC conductor is in one of the large poloidal coils required in a fusion reactor. [3],[4],[5],[6]

The remainder of the report is organized into the following categories: Experimental Parameters and Facilities, Experimental Procedure, Results, Conclusions and Recommendations, and an Appendix. 'Experimental Procedure' includes the results of the inductive heater verification test. 'Results' concerns four main topics: 1)effect of mass flow rate on stability; 2)effect of changing experimental parameters on stability, including immersing the conduit in helium versus surrounding it by vacuum; 3)effect of heating duration on stability; and 4)the pressure rise following a quench, including how the magnitude and appearance of such pressure rises changes with an imposed mass flow. The Appendix includes information about the original goal of this study, which was to determine how stability varies with varying cooled conductor perimeter. A detailed analysis of the results will be presented in a later report.

## 2. Experimental Parameters and Facilities

All of the tests were performed at JAERI's Superconducting Magnet Laboratory, located in the Naka Fusion Research Establishment. The test coil was a cable-in-conduit NbTi coil. Its parameters are listed in Table 1, while a photograph of the coil, a microphotograph of the conduit cross-section and the strand cross-section, and a front and side view sketch are given in Figs. 1 - 3, respectively. It is important to note that the conduit was not impregnated with epoxy. Fig. 4 shows how the insulation between turns was provided by FRP inserts.

The helium boxes indicated in Fig. 3 are cylindrical enclosures designed to offer the test coil a readily accessible helium inventory. Each box contained approximately 1750 cubic centimeters of 4.2 K supercritical helium. The pressure taps, two of which measured the pressure of the boxes, were connected to the pressure transducers by stainless steel tubes leading from the swagelock fittings to room temperature outside of the cryostat. The time delay of the diaphragm-type transducers was at least 100 msec, thus rendering any kind of transient pressure measurement impossible.

Fig. 5 is a schematic giving the locations of the voltage and pressure taps, the inlet and outlet thermocouples, the thin-film carbon temperature sensors, and the resistive and inductive heaters. The carbon temperature sensors were attached to the outside of the conduit wall with epoxy, which also served as insulation. The time delay of these sensors, not including the time required for heat to be conducted through the conduit wall, is about 1 msec. A rough calculation for that conduction time gives a number on the order of 10 microseconds.

The inductive heaters were constructed from 0.4 mm diameter, formvar-coated copper wire. The wire was wound around the outside of the conduit (125 turns). The arc length of each heater was 55 millimeters.

As can be seen in the photograph of Fig. 6 and the sketch of Fig. 7, the sample coil was inserted in a pool-cooled background field coil of 240 mm inner bore, which generated the 7 T field under which the data were taken. The electric circuits of both coils are schematically shown in Fig. 8. The supercritical helium supply system, which operated on a simple pressure-differential concept, is given in Fig. 9. Finally, the data acquisition system, consisting of both digital storage and strip chart recorders, can be seen in Fig. 10.



Table 1 Test Coil Parameters

|                   |                         |                                     |
|-------------------|-------------------------|-------------------------------------|
| <u>COIL</u>       | Type                    | force-cooled cable-in-conduit       |
|                   | Insulation              | FRP spacers between turns; no epoxy |
|                   | Length                  | 8 m                                 |
|                   | No. of Turns            | 10                                  |
|                   | Inner Diam.             | 179 mm                              |
|                   | Outer Diam.             | 200 mm                              |
|                   | Height                  | 174 mm                              |
|                   | No. of Cooling Channels | 1                                   |
|                   | Design Current          | 2.4 kA                              |
|                   | Design Field            | 7 T                                 |
|                   | Self Inductance         | $1.57 \times 10^{-5}$ H             |
|                   | <u>COOLANT</u>          | supercritical helium                |
| Inlet Pressure    |                         | 5 - 6 atm                           |
| Inlet Temperature |                         | 4.2 K                               |
|                   |                         |                                     |
| <u>CONDUIT</u>    | Material                | SUS 304                             |
|                   | Outer Dimensions        | 10.8 x 10.8 mm                      |
|                   | Thickness               | 1.1 mm                              |
| <u>CONDUCTOR</u>  | Type                    | multifilamentary NbTi               |
|                   | Void Fraction           | 45.8 %                              |
|                   | Twist Pitch             | 103 mm                              |
|                   | $A_{Cu}$                | 23.97 mm <sup>2</sup>               |
|                   | $A_{NbTi}$              | 5.42 mm <sup>2</sup>                |
|                   | $A_{CuNi}$              | 9.32 mm <sup>2</sup>                |
| <u>STRAND</u>     | Diameter                | 2.03 mm                             |
|                   | Number                  | 12                                  |
|                   | Filament Diam.          | 20.6 micrometers                    |
|                   | No. of Filaments        | 1344                                |
|                   | $A_{Cu}$                | 1.998 mm <sup>2</sup>               |
|                   | $A_{NbTi}$              | 0.777 mm <sup>2</sup>               |
|                   | $A_{CuNi}$              | 0.452 mm <sup>2</sup>               |
|                   | Twist Pitch             | 17.4 mm                             |
| <u>SUBCABLE</u>   | Number                  | 4                                   |
|                   | No. of strands          | 3                                   |
|                   | Twist Pitch             | 42 mm                               |

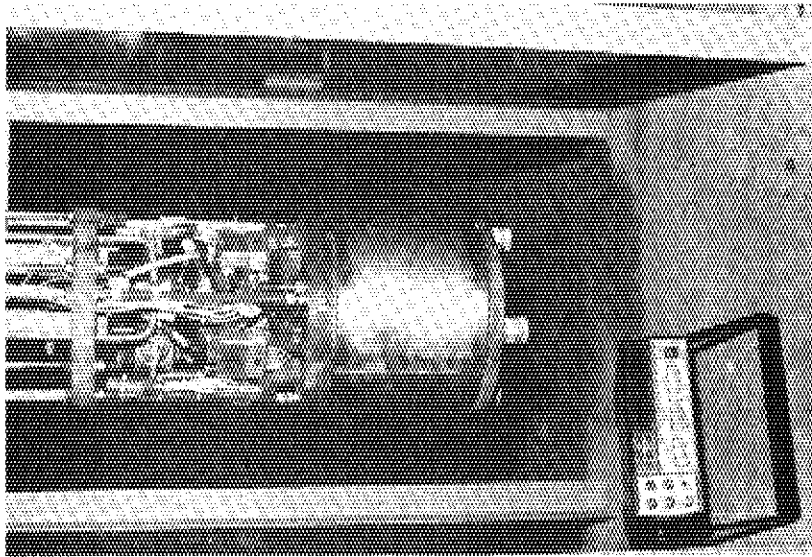
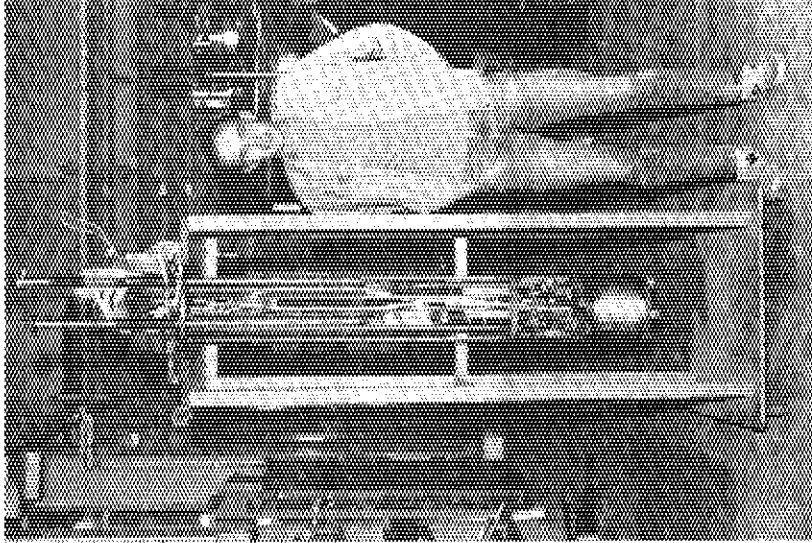
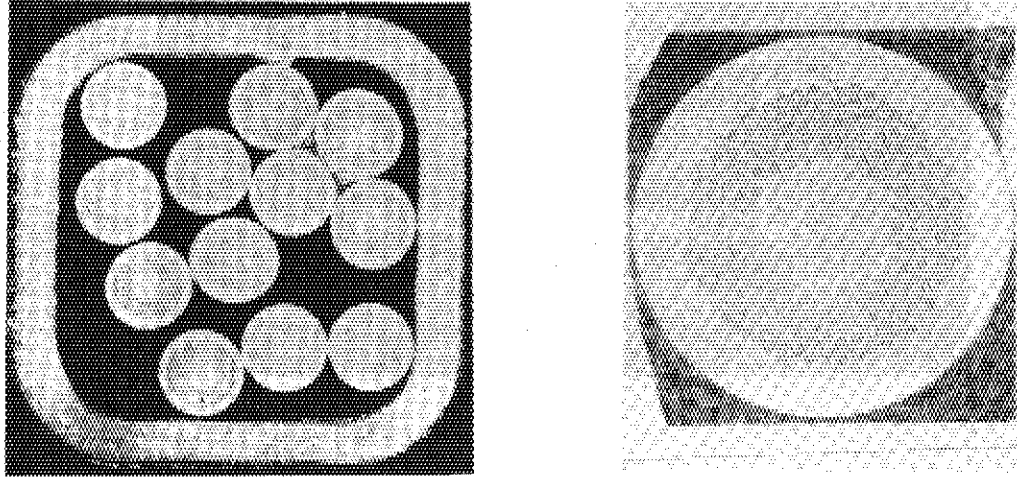


Fig. 1 Photographs of the Sample Coil



**Fig. 2 Microphotographs of the Conduit and Strand  
Cross-Sections**

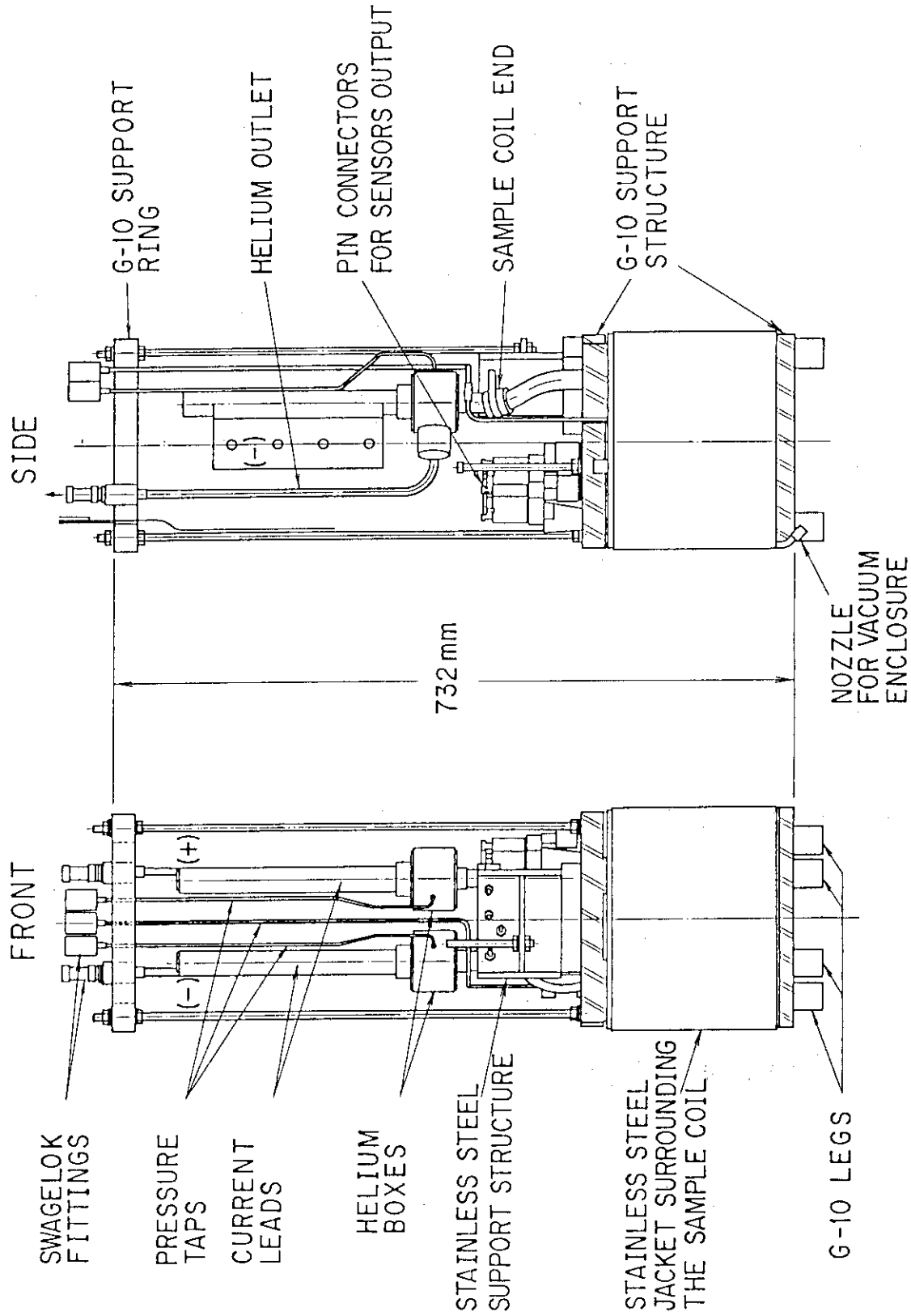
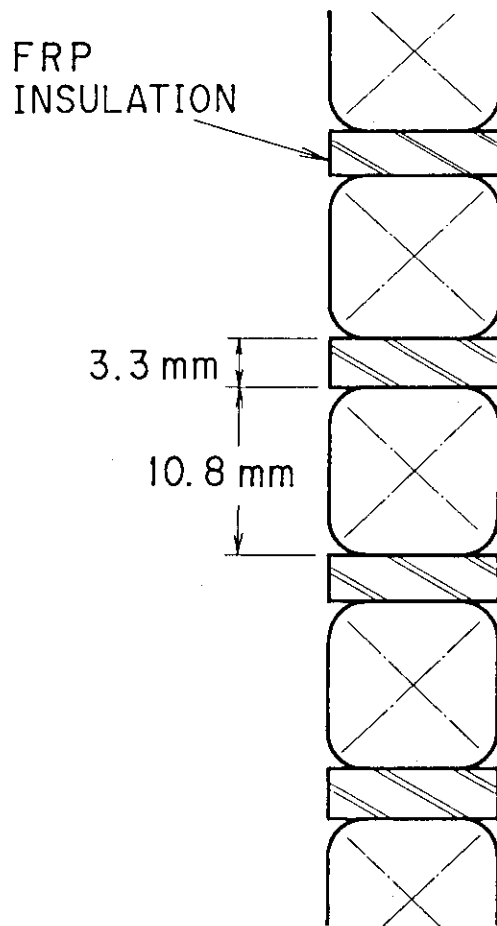


Fig. 3 Sample Coil: Front and Side Views



NOTE : THE CONDUIT IS NOT COVERED WITH EPOXY.

**Fig. 4 Insulation Between Turns**

SYMBOLS

- PI, P2, P3 PRESSURE TAPS
- VJ, VK VOLTAGE TAPS
- TCJ, TCK THERMOCOUPLES
- TH1, TH2 ..... CARBON THIN-FILM RESISTORS
- STH1, STH2 ..... RESERVE CARBON THIN-FILM RESISTORS
- IH1, IH2 ..... INDUCTIVE HEATERS
- RH1, RH2 RESISTIVE HEATERS

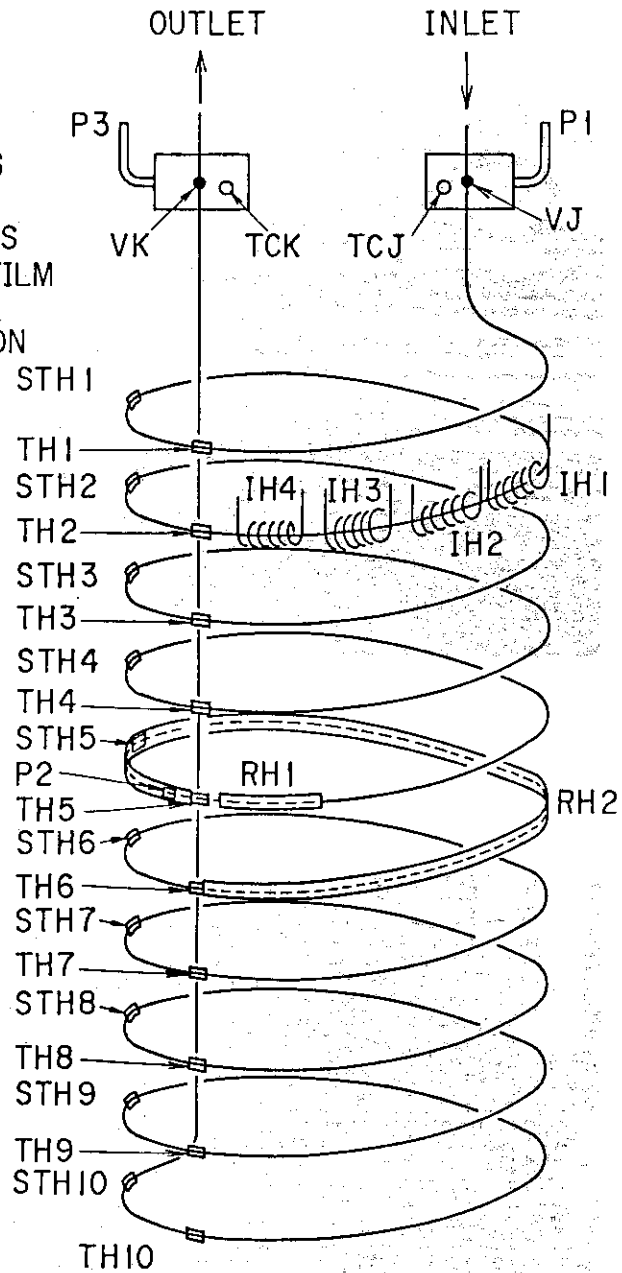


Fig. 5 Schematic of Sensor and Heater Locations

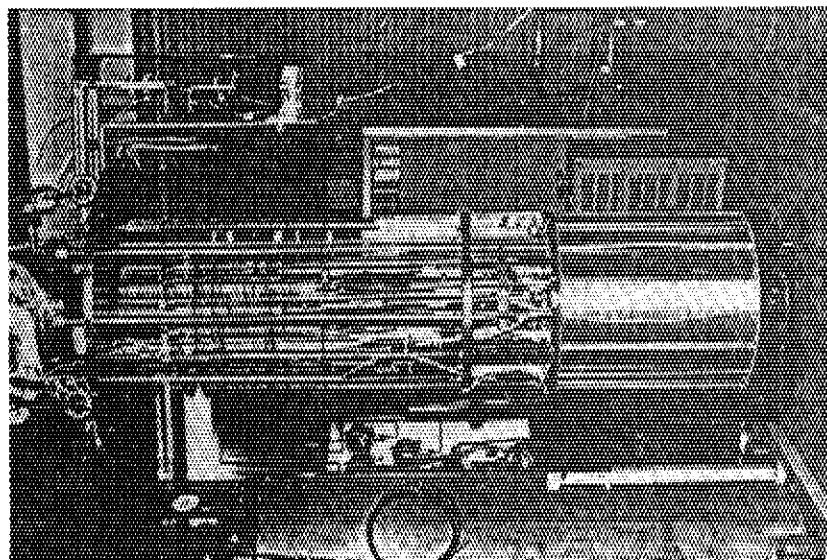
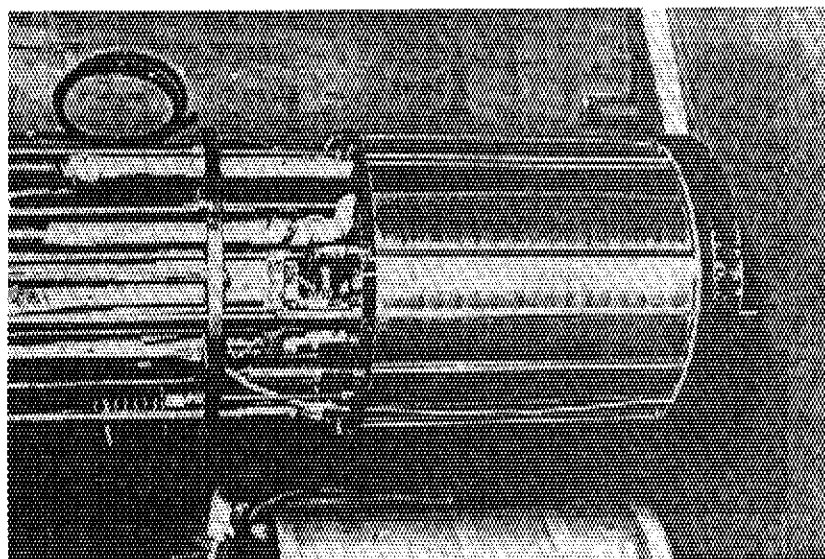


Fig. 6 Photographs of the Sample Coil Inside of the Background Field Coil

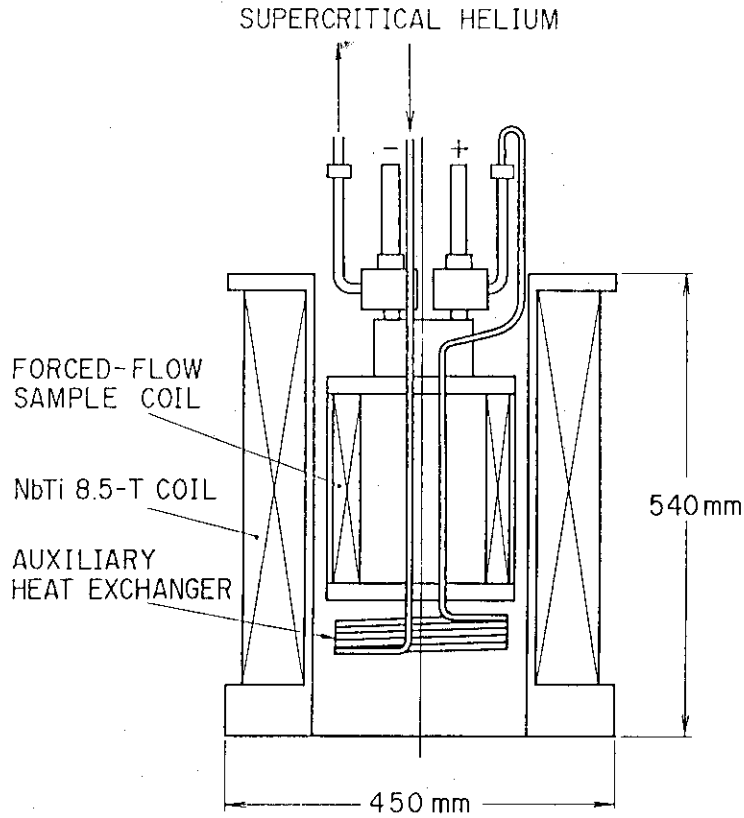
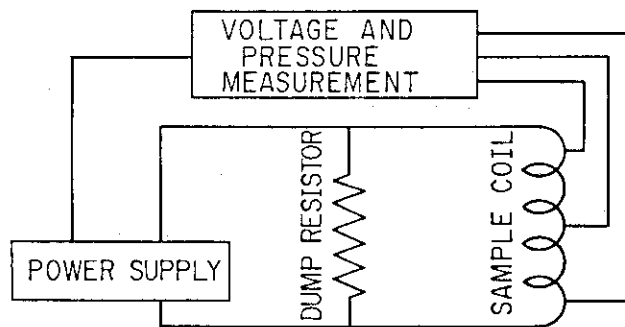
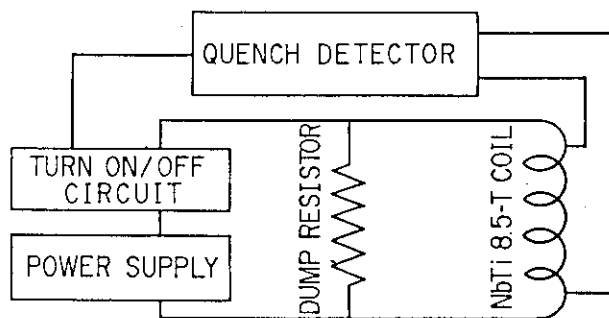


Fig. 7 Sketch of the Sample Coil Inside of the Background Coil



SAMPLE COIL ELECTRIC CIRCUIT



BACKGROUND FIELD COIL ELECTRIC CIRCUIT

Fig. 8 Electrical System



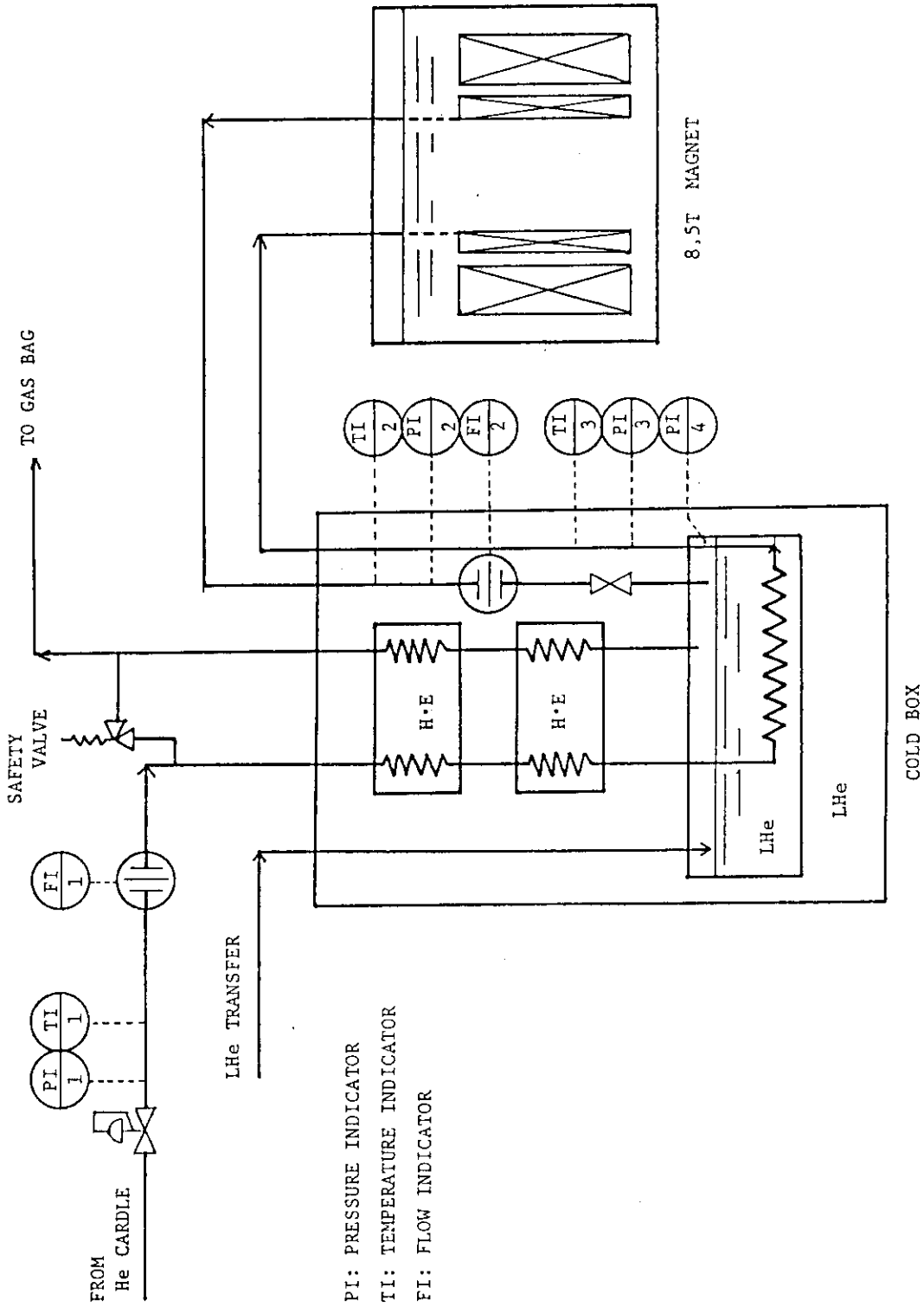


Fig. 9 Supercritical Helium Supply System

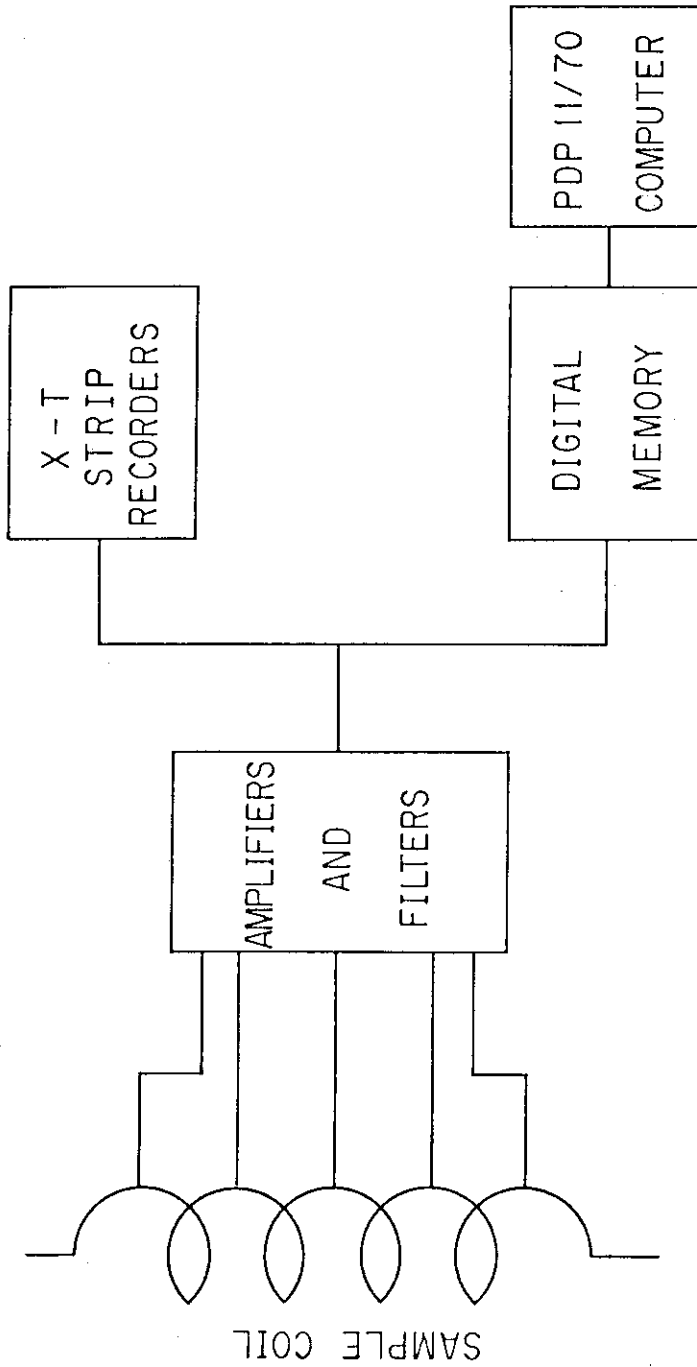


Fig. 10 Data Acquisition System

### 3. Experimental Procedure

Three sample coils were initially available for experimentation: Coil A, Coil B, and Coil C. The original purpose of this study was to compare the stability characteristics of the coils so as to determine the relationship between conductor cooled perimeter and stability (the coils were nearly equivalent in every other parameter). Since Coil A had already been tested before the author's arrival, only B and C remained to be investigated. After the second test of Coil B, however, it was found that Coil C was defective, thus leaving only A and B for comparison. Such a comparison, though, was not considered satisfactory since A had only been equipped with resistive heaters and it was felt, for reasons described in the Appendix, that resistive heat input held little meaning with regard to stability. It was therefore decided to test Coil B for a third time, emphasizing stability under flow rate conditions rather than the original goal of comparing stability under varying conductor perimeter. This third experiment didn't produce any data due to a failure of the current leads, but the fourth and final test did.

Each experiment was carried out at a background field of 7 T, at an inlet temperature of 4.2 K, and at an inlet pressure ranging between 5.1 and 6.1 atm. The pressure variation was not intentional. These conditions were selected so that the data could be more directly compared with those of Coil A. In addition, a 28 msec resistive heating duration was chosen for the same reason.

Coil B's first test took place under the condition that a vacuum space surrounded the outside of the conduit. Data from both inductive and resistive input were obtained, all under zero-flow conditions. A curious phenomenon, at the time termed "resistive quenching", occurred at irregular intervals while using an inductive heater: a quench would be initiated one to two seconds after heating, instead of the usual nearly simultaneous quench if the heat input was sufficient. It was thought that such a quench was due to the inductive heater becoming warm enough to act as a resistive heater, bringing about the much delayed quench. The solution seemed to be simple: introduce liquid helium to the outside wall of the conduit so that the heater would be quickly cooled after every use.

The second test was carried out under such conditions. It was quickly discovered that the presence of helium outside of the conduit had little effect on the "resistive quenching"; this phenomenon still occurred at irregular intervals and at various heater currents. Data taken during the second test once again included only zero-flow data, with both resistive and inductive input.

As previously mentioned, both the first (and only) test of Coil C and the third test of Coil B produced no data. The fourth

experiment generated data under zero, 1.2, and 2.4 g/sec flow rates. Only an inductive heater was used. The previous experimental error which led to the "resistive quenching" was finally discovered: the waiting period between data points during tests one and two was insufficient. That duration was only two to four minutes, as compared to the approximately ten minutes of the fourth test. No "resistive quenches" occurred. It is assumed that the short waiting times led to unsteady initial conditions--especially the conductor and helium temperatures and the helium pressure. With these parameters slightly higher than normal, a situation could have existed where a quench at a given heat input would only occur under such an elevated temperature and pressure. At any rate, further thought will be given to this problem.

The inductive heater power supply produced waveforms similar to those shown in Fig. 11. Only results from the 1/2 wave, 0.44 msec and the two cycle, 2.1 msec inputs (both at a frequency of 1560 Hz) are presented in this report, although a few longer and lower frequency data points were taken in the first test. The heat input to the conductor, in mJ/cc strand, was calculated by a computer program which took into account the axial variation of magnetic field. The program employed the code FORCE [7] for calculation of the magnetic field inside the conductor. Since the skin depth at 1560 Hz, about 0.27 mm, and the thickness of the copper surrounding the NbTi filaments (refer to Fig. 2) was nearly equivalent, the calculation assumed that the conductor was entirely copper.

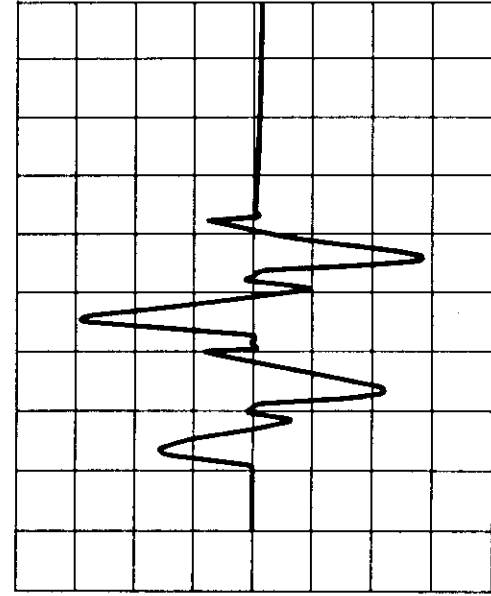
Two inductive heater verification tests were conducted. In the first, three thermocouples were attached to an 8 mm long copper wire of 2.0 mm diameter, the whole of which was then covered with epoxy. The test heater was 10 mm long. The results of this test are given in Table 2. A transient heat transfer coefficient

$$h = (k \times \rho \times c_p / t)^{0.5}$$

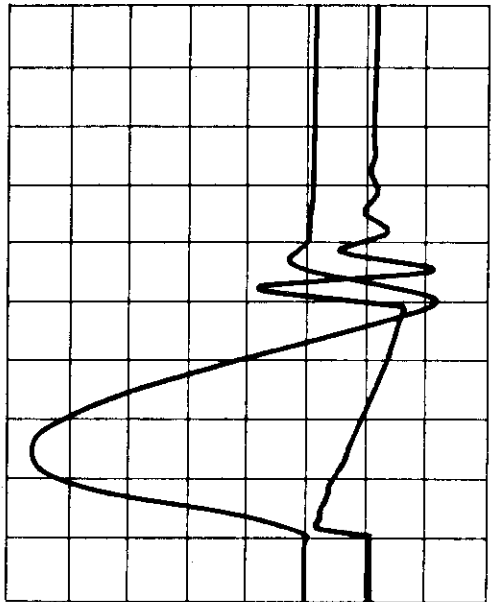
where  $h$  = transient heat transfer coeff. [ $W/(m^2 \times K)$ ]  
 $k$  = thermal conductivity of epoxy [ $W/(m \times K)$ ]  
 $\rho$  = density of epoxy [ $Kg/m^3$ ]  
 $c_p$  = specific heat of epoxy [ $J/(Kg \times K)$ ]  
 $t$  = time [sec]

was used to account for the heat conducted to the epoxy. This coefficient was calculated to be about  $2000 W/(m^2 \times K)$  and was considered to be constant for all temperatures. For copper, a constant density, a variable specific heat (function of temperature only), and a resistivity which varied with background magnetic field were assumed. Both verification tests took place under zero background field.

The second test was attempted because a verification test where the sample would be surrounded by vacuum was desired. Once again three thermocouples were attached to the sample, which this



2.1 msec pulse  
heater current  
0.5 msec/div



0.44 msec pulse  
upper trace: heater current  
lower trace: heater voltage  
0.1 msec/div

Fig. 11 Inductive Heater Waveforms

Table 2 Results From the First Inductive Heater Verification Test

| Shot No. | Final Temp. (K) | Measured Energy Input (mJ/cc Cu) | Calculated Energy Input (mJ/cc Cu) | % Diff. |
|----------|-----------------|----------------------------------|------------------------------------|---------|
| 7        | 10.5            | 159                              | 148                                | -7.4    |
| 8        | 7.5             | 39.8                             | 51.6                               | 22.9    |
| 9        | 8.4             | 62.1                             | 74.5                               | 16.6    |
| 10       | 9.3             | 93.9                             | 118                                | 20.4    |
| 11       | 10.3            | 146                              | 155                                | 5.8     |
| 12       | 11.3            | 221                              | 200                                | -10.5   |

Note: A total of 13 shots were taken during this test. The shots not presented were either not recorded into the digital memory, the power input was too small for the resolution of the thermocouple output, or some problem occurred with the heater power supply.

time was only 4 cm in length. After a few data points were taken at 0.1 torr vacuum, the heater power supply malfunctioned, making any further points at lower vacuum pressures impossible. Since the 0.1 torr data indicated a temperature rise significantly less than what would be expected under adiabatic conditions, the vacuum was deemed insufficient for adiabatic simulation. Thus, only results from the first test in epoxy can be considered.

The maximum percent difference between the energy input calculated from the computer code and that calculated from the thermocouple output is 22.9 %. This is considered to be an acceptable difference when taking into account the resolution of the thermocouple output voltage and the resolution of the input heater current. Values calculated from the computer program are therefore taken to be correct.

## Results

Due to the lack of time between completion of the experiments and the writing of this report, the results are presented mostly without comment. A detailed analysis will be published in the future.

### Effect of Mass Flow Rate on Stability

Flow rates of 0, 1.2, and 2.4 g/sec, corresponding to helium velocities of 0, 24, and 48 cm/sec, were tested. As indicated in Fig. 12, an imposed flow substantially increased the stability before 3.0 kA operating current. Similar results are reported in Refs. 5, 8, and 9. It is apparent that a large region of multi-valued stability is present at zero imposed helium, but that region is reduced at 1.2 g/sec and disappears at 2.4 g/sec, once again much like the results of Ref. 5.

Fig. 13 gives the maximum stable current versus helium flow rate at heater inputs of 100, 200 and 300 mJ/cc st. If one squares the maximum stable current and calculates its power dependence on mass flow rate

$$(I_{\max})^2 = C \times (m_{\text{He}})^n + A$$

where  $I_{\max}$  = maximum stable current [kA]  
 $m_{\text{He}}$  = helium mass flow rate [g/sec]  
 $n$  = exponent  
 $C, A$  = constants

the result is 0.98, 0.63, and 0.63 for  $n$  for energy inputs of 100, 200 and 300 mJ/cc st, respectively. The average of these exponents is 0.75, which is almost the same as the exponent of the Reynolds' number in the Dittus-Boelter correlation for a steady-state convective heat transfer coefficient (0.8).

Fig. 14 is the temperature history, calculated from the stability code ALPHE II [10], of both the conductor and the helium for a different sample coil. [11] It is seen that after the end of the input heat pulse, which occurs at the peak of the conductor temperature, the helium and the conductor equilibrate at a common temperature, which remains more or less constant for a period of at least several milliseconds. This tendency is supported by independent experimental results. [12] It is thought that imposed mass flow is instrumentative in determine the magnitude of the equilibrium temperature, but that the maximum temperature of the conductor depends only on transient conduction and not on imposed mass flow. Also, mass flow rate could effect the length of time during which the equilibrium temperature remains above the ambient temperature. Thus, the influence of mass flow rate could approach the steady-state dependence of the Dittus-Boeltner correlation provided that the equilibrium "hot" state remains for a long enough period of time.

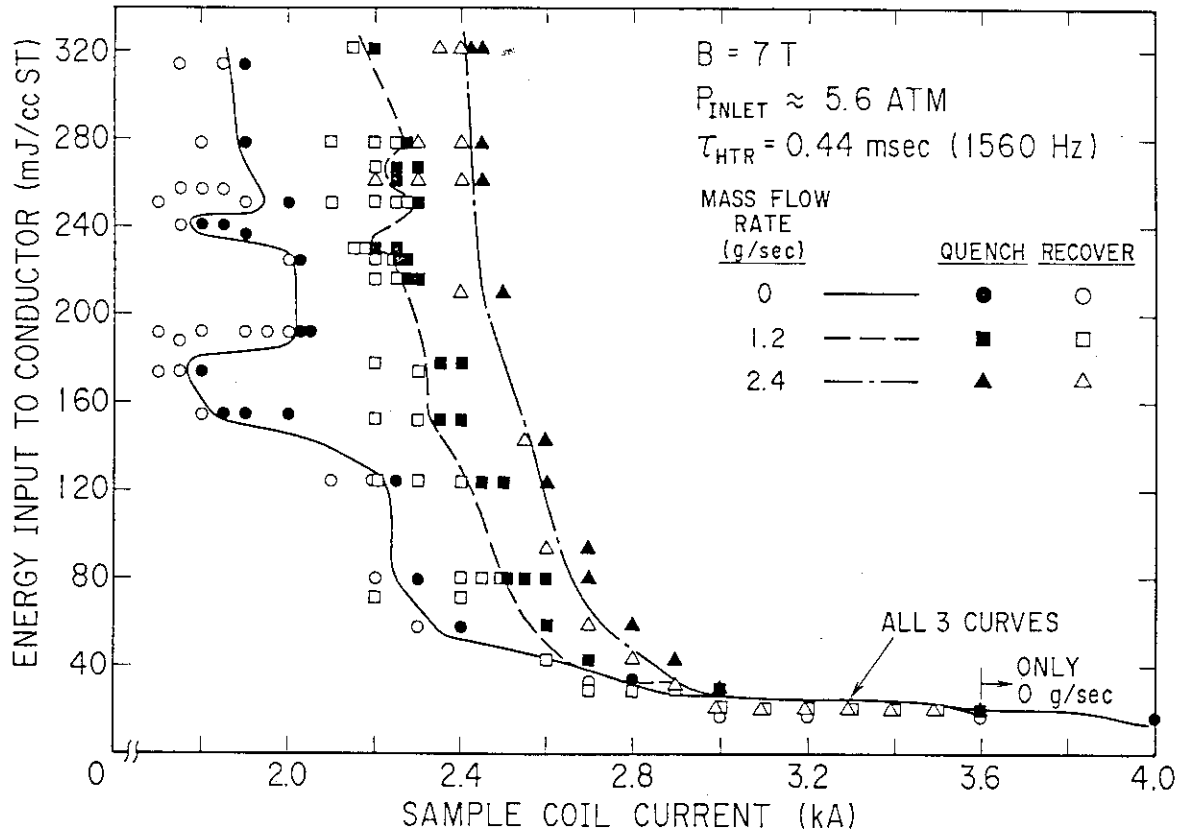


Fig. 12 Stability vs. Coil Current at Varying Flow Rates

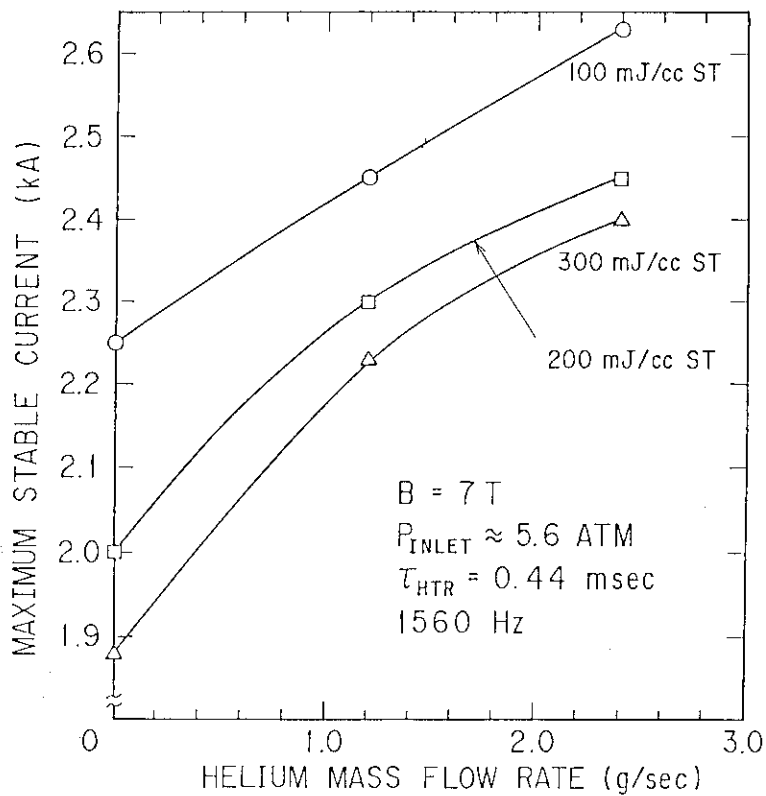
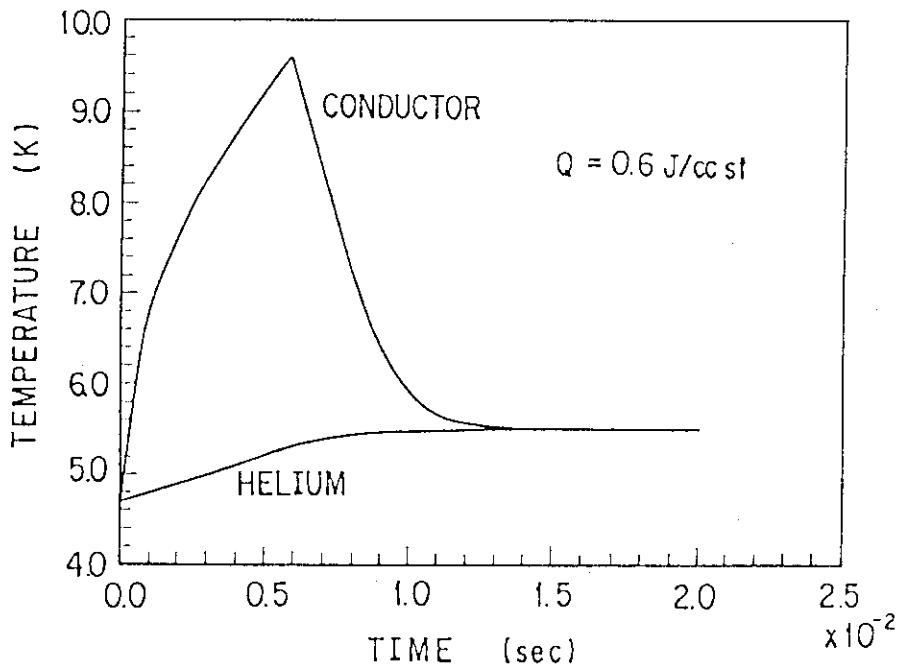
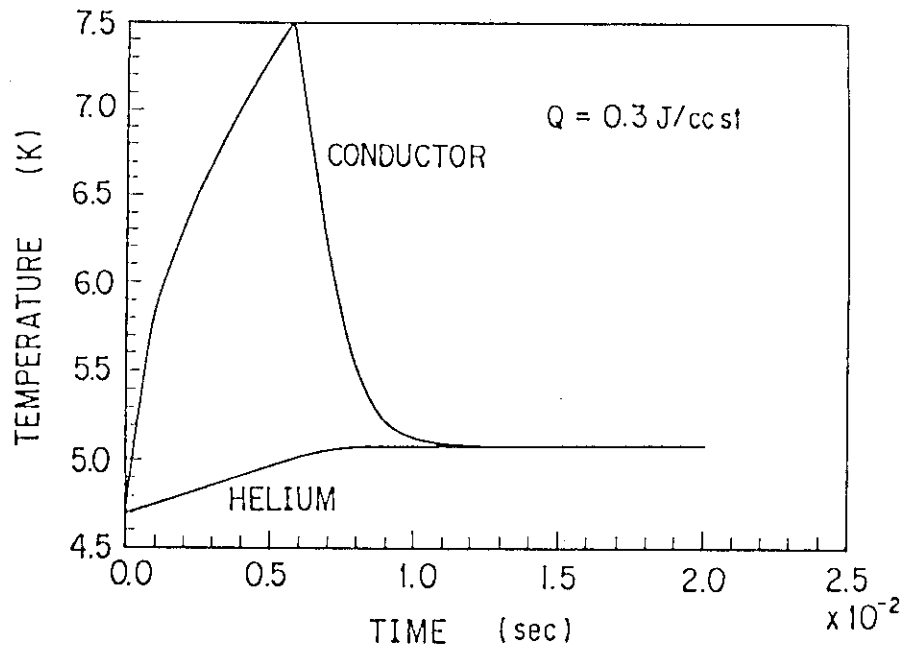


Fig. 13 Maximum Stable Current vs. Mass Flow Rate at Varying Energy Inputs

Note: Drawn Curves Are Not the Result of a Calculation





**Fig. 14** Calculated Conductor and Helium Temperature History from Ref. 11

## Repeatability of Results

Zero-flow stability varied widely between the three tests of the sample coil. Fig. 15 is an indication of the magnitude of the variation. It is important to note that the data taken on 8/1/86 were obtained while the conduit was surrounded by a vacuum, whereas the other two sets of data from 10/31/86 and 12/10/86 were obtained while the conduit was surrounded by atmospheric pressure liquid helium. The outside helium has no direct influence on transient stability. It seems that the experimental parameters of initial pressure and temperature play a more important role. It is thought that the absence of a limiting current in the 8/1/86 data is due to an insufficient number of data.

## Effect of Heating Duration on Stability

The data presented in Fig. 16 were taken during the second test. The dotted line, representing points taken during 2.1 msec heating, is left unfinished in the center of the graph because of the confusing nature of the data. It is clear that some kind of multi-valued stability must be present, but not enough points were taken to accurately map the stability. A preliminary conclusion concerning this graph is that the length of heat pulse plays a very important role before the limiting current ( $I_{lim}$ ), but not after. A reason could be the effective length that heat is able to diffuse from the conductor through the helium. Before  $I_{lim}$ , the induced velocity enables heat to be rapidly transported by a convective process. After  $I_{lim}$ , heat transport is mostly dependent on a transient conduction process. The effective length of diffusion is therefore limited by the thermal diffusivity of helium. A simple calculation of this length

$$D_{He} = (DIFF \times DUR)^{1/2}$$

where  $D_{He}$  = effective length of diffusion [m]  
 DIFF = helium thermal diffusivity [ $m^2/sec$ ]  
 DUR = heating duration [sec]

gives about 5 microns for 0.44 msec heating and about 10 microns for 2.1 msec heating. These numbers can be compared with a value of 30 microns, estimated from 2 msec heating, 10 atm helium experimental results. [12] Thus, the large difference in stability before  $I_{lim}$  can be explained by the large difference in the effective lengths of diffusion (making available a much larger volume of helium for cooling in the 2.1 msec case), whereas in a similar vein the very small or nonexistent difference in stability after  $I_{lim}$  can be explained by the very small effective lengths of heat diffusion, in which the volume of helium available for cooling is only slightly different between 0.44 msec and 2.1 msec heating and not enough to make an observable difference.

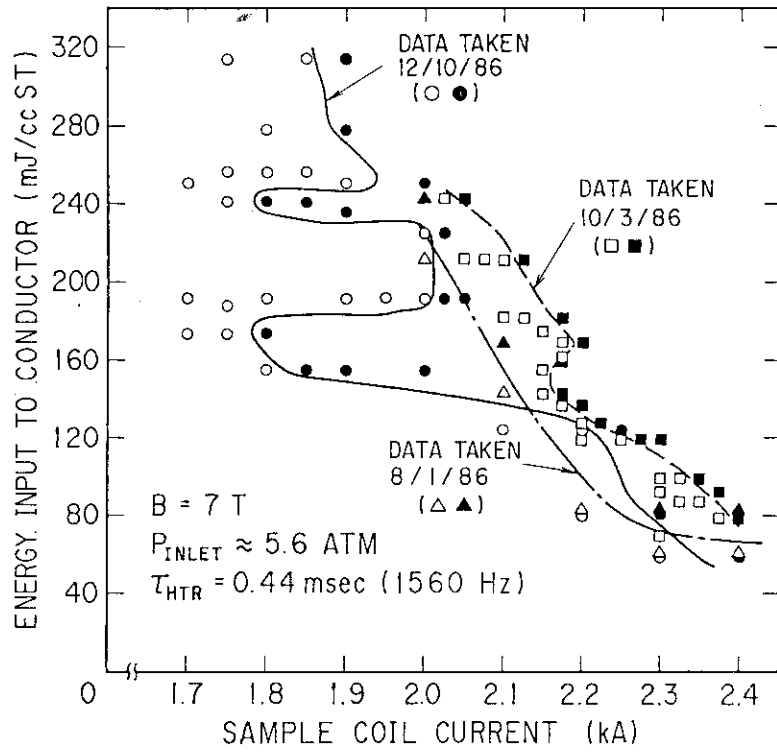


Fig. 15 Zero-flow Stability Measured on Three Occasions

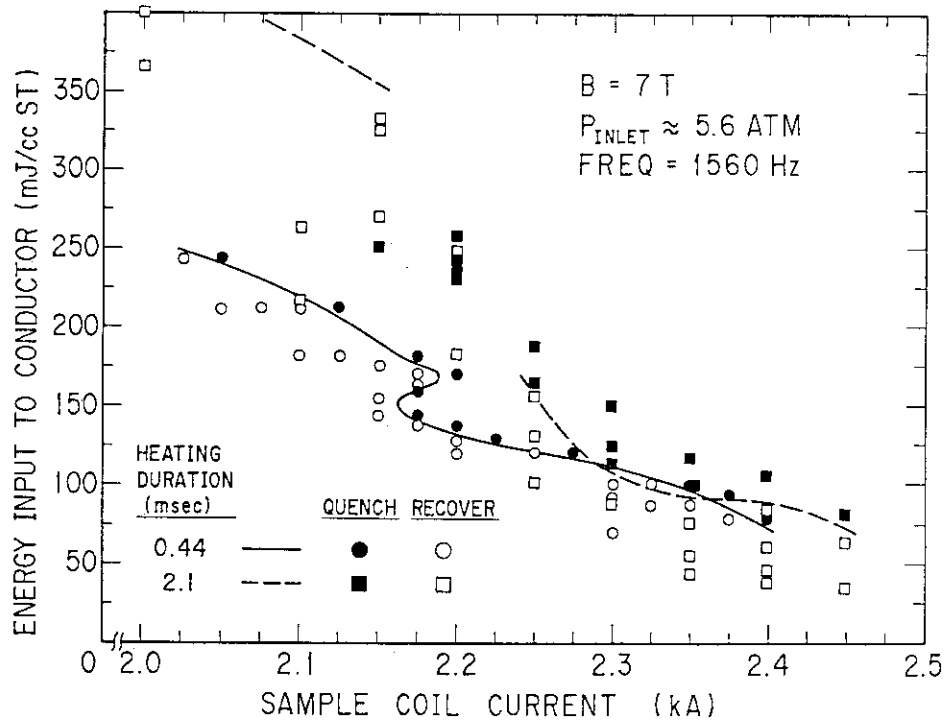


Fig. 16 Stability vs. Coil Current for Two Heating Durations

\*  
Pressure Rise Following a Quench

Quench-induced pressure rises were investigated by delaying the downramping of the sample coil current so that the magnitude of such pressure rises, with and without imposed mass flow rates, could be determined. It was found that an imposed helium flow drastically altered the magnitude and the appearance of quench-induced pressure rises. Figs. 17 and 18 are typical examples. Fig. 19 is an attempt to describe the dependence of pressure rise on mass flow rate. The only tentative conclusion which has been reached so far is that the mass flows employed (1.2 and 2.4 g/sec) reduced the pressure rise after 2.1 sec by a factor of 3. Some caution is advised, however, before completely accepting this statement since the decreased pressure could depend more on the changed boundary conditions during flowing conditions; for example, an open outlet valve is used for flowing conditions versus a closed outlet valve for zero flow rate. Anyway, a direct correlation between flow rate and pressure rise cannot be reached because of the conflicting data presented in Fig. 19. The pronounced dips in the curves in Fig. 18 have not been explained yet.

An approximate squared dependence of pressure rise on sample coil current is displayed in Fig. 20. Such a dependence is expected for the zero-flow data.

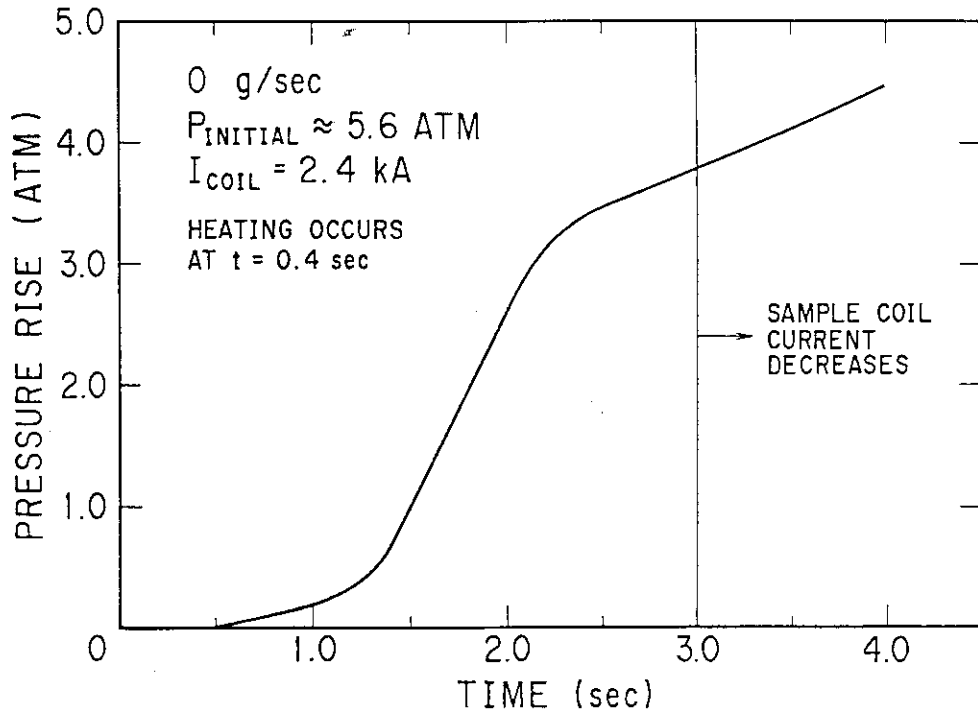


Fig. 17 A Typical Quench-Induced Pressure Rise at Zero Imposed Mass Flow

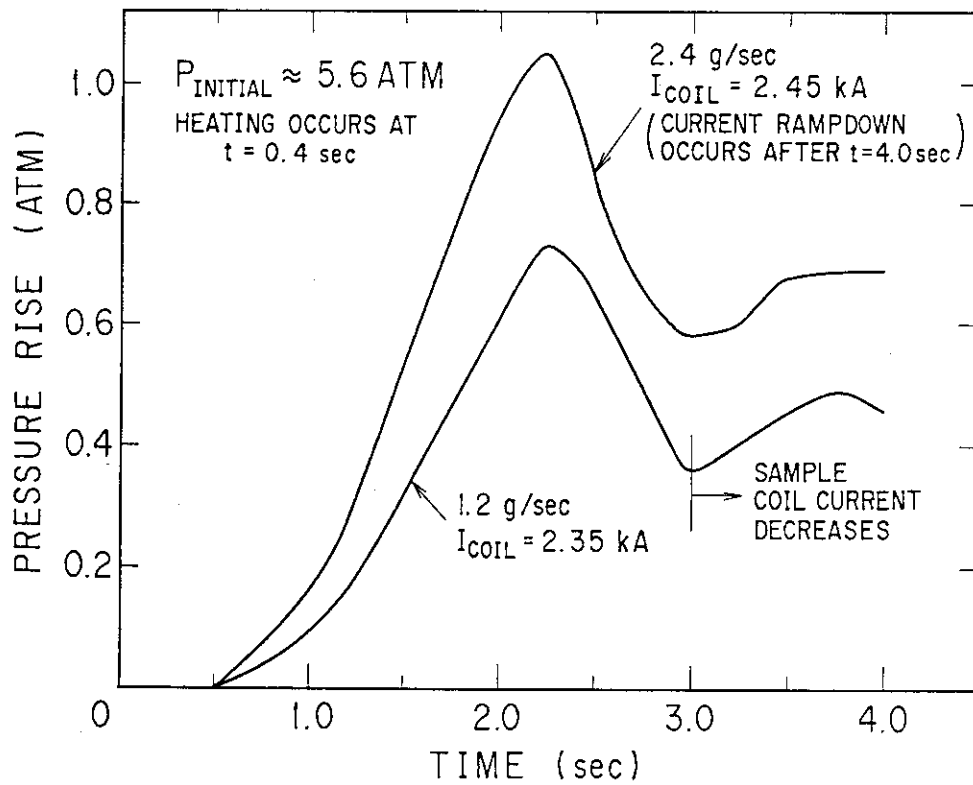


Fig. 18 Two Typical Quench-Induced Pressure Rises Under Imposed Mass Flows

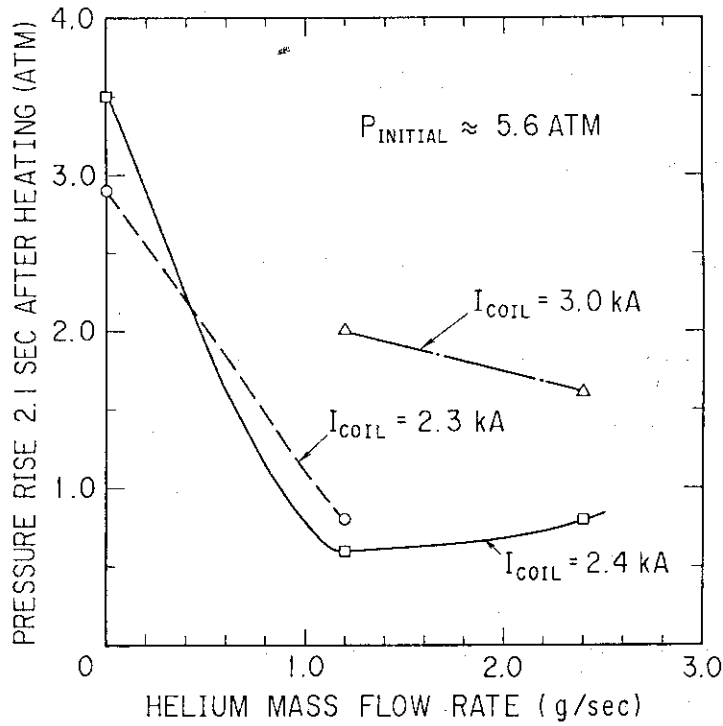
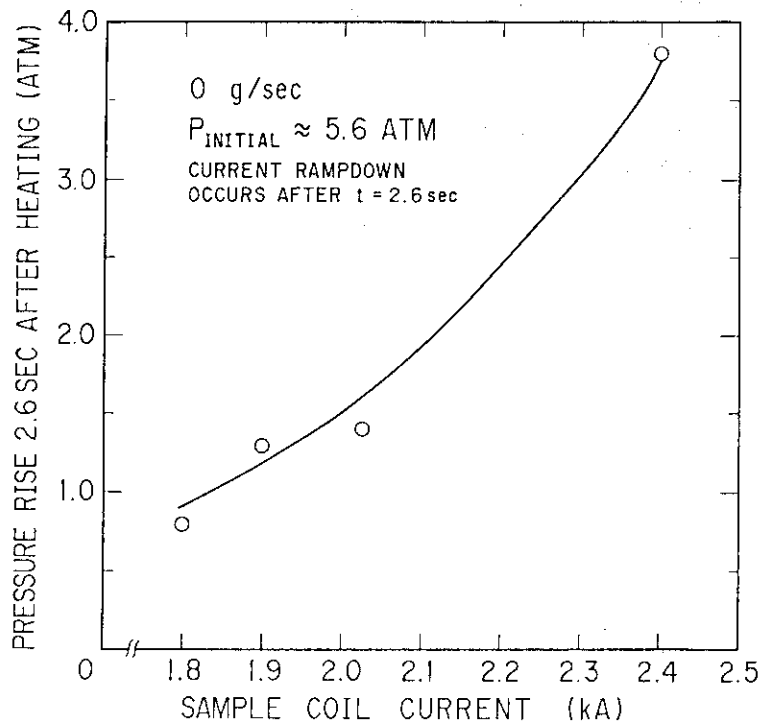


Fig. 19 Influence of Imposed Mass Flow on Quench-Induced Pressure Rises

Note: Drawn Curves Are Not the Result of any Calculation.



Note: The Drawn Curve Is Not the Result of any Calculation.

Fig. 20 Zero Flow Quench-Induced Pressure Rise as a Function of Sample Coil Current

## 5. Conclusions and Recommendations

Conclusions reached at this point in the analysis can be summed up as:

1) An imposed mass flow rate substantially increases the stability margin.

2) The presence of helium outside of the conduit versus a vacuum surrounding the conduit has no discernible effect on transient stability.

3) An increase in heating duration before the limiting current significantly increases the stability margin, but there is little effect after  $I_{lim}$ .

4) Tentatively, an imposed mass flow decreases the pressure rise following a quench, compared with a pressure rise during a zero imposed mass flow, by about a factor of three after two sec. The shape of the mass flow-pressure rises shows a prominent dip which has not yet been explained.

Recommendations include the following:

1) refitting the sample coil (or perhaps a future coil) with more temperature sensors, pressure taps, and voltage taps near the heaters so that more can be known about the heated zone. In addition, an accurate measurement of induced velocity and transient pressure rise is required.;

2) varying the heating duration in the range from 0.1 msec to 1.0 msec to determine if the "effective diffusion length" concept expressed earlier is valid; and

3) varying the length of the heated zone.

## APPENDIX

Effect of Varying Cooled Perimeter on Stability

Very little information about this topic can be deduced from the results. If the study had gone as planned, more definitive statements could be made with regard to cooled perimeter's impact on stability. The pertinent parameters of the original three coils, Coil A, Coil B, and Coil C, are listed in Table 3. All parameters not given are approximately equal for each coil.

The only directly comparable data is presented in Fig. 21. As mentioned earlier, Coil A had been equipped with only resistive heaters; thus, only resistive input can be compared. The construction of the resistive heaters, however, casts doubt about the usefulness of Fig. 21. As can be seen in Fig. 22, the resistive heaters are located on the outside of the conduit wall, resulting in the situation where the heat first enters the conduit, conducts through to the helium, heats up the helium, and finally comes into contact with the conductor. Such an arrangement can be shown to be impractical by considered a simple case where a long cylindrical rod at 4.2 K is immersed in a relatively hot fluid bath at 7 K, which represents the hot helium during resistive heating. The value of 7 K was chosen by first picking from Fig. 22 the measured stability margin of 1.5 J/cc He at 1.0 kA, multiplying by the density of helium at 4.2 K and 6.0 atm, adding the result to the enthalpy of helium at 4.2 K and 6.0 atm, and finally determining what temperature corresponded with the final enthalpy. According to the theory in Ref. 13, the temperature history of the rod can be easily ascertained if the rod's Biot number is less than or equal to 0.1. The Biot number is calculated by

$$Bi = h_o r_o / k$$

where  $Bi$  = Biot number (dimensionless)  
 $h_o$  = convective heat transfer coefficient [W/(m<sup>2</sup> K)]  
 $r_o$  = radius of the rod (m)  
 $k$  = thermal conductivity of the rod [W/(m K)]

For this simple analysis both  $h_o$  and  $k$  are assumed to be constant:

$$k = 1000 \text{ W/m K} \quad [1]$$

$$h_o = 1000 \text{ W/m}^2\text{K} \quad [14]$$

If we take the conductor strands to be one large rod with a total perimeter equivalent to the sum of the individual strands' perimeter, the largest Biot number corresponds to the rod with the largest perimeter and therefore the largest radius. That value, which is the Biot number for Coil C, is about 0.04. Thus, a "lumped" approximation is valid.

The results of the "lumped" analysis are displayed in Fig. 23. A unit length of the rod, with corresponding wetted surface areas of 0.133 m<sup>2</sup>, 0.077 m<sup>2</sup>, and 0.231 m<sup>2</sup>, for Coil A, Coil B, and Coil C, respectively, is considered to be immersed. The



Table 3 Parameters of the Three Original Sample Coils

|        | STRAND<br>DIAMETER<br>(mm) | NUMBER<br>OF<br>STRANDS | TOTAL<br>CONDUCTOR<br>PERIMETER<br>(mm) |
|--------|----------------------------|-------------------------|---|
| COIL A | 1.18                       | 36                      | 133                                     |
| COIL B | 2.03                       | 12                      | 77                                      |
| COIL C | 0.68                       | 108                     | 231                                     |

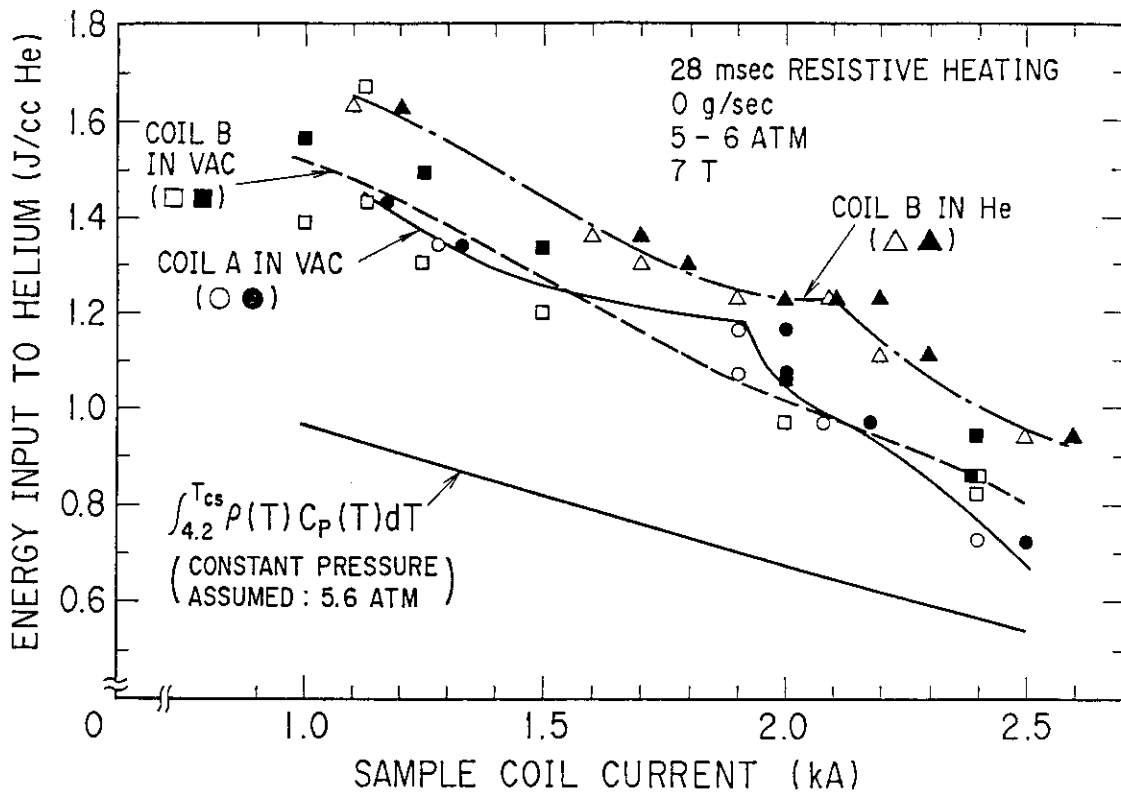


Fig. 21 Stability Under Resistive Heating

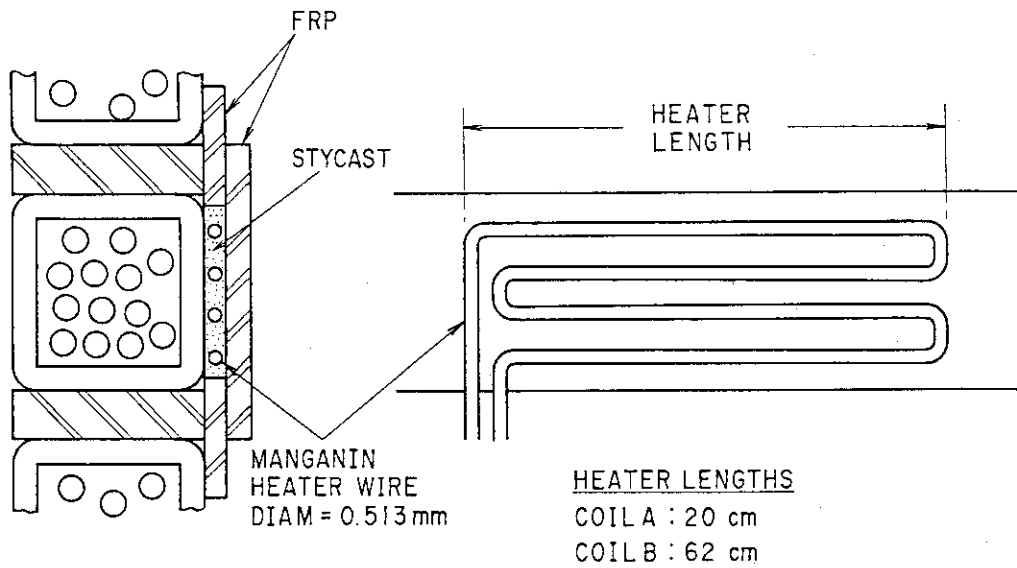


Fig. 22 Resistive Heater Configuration

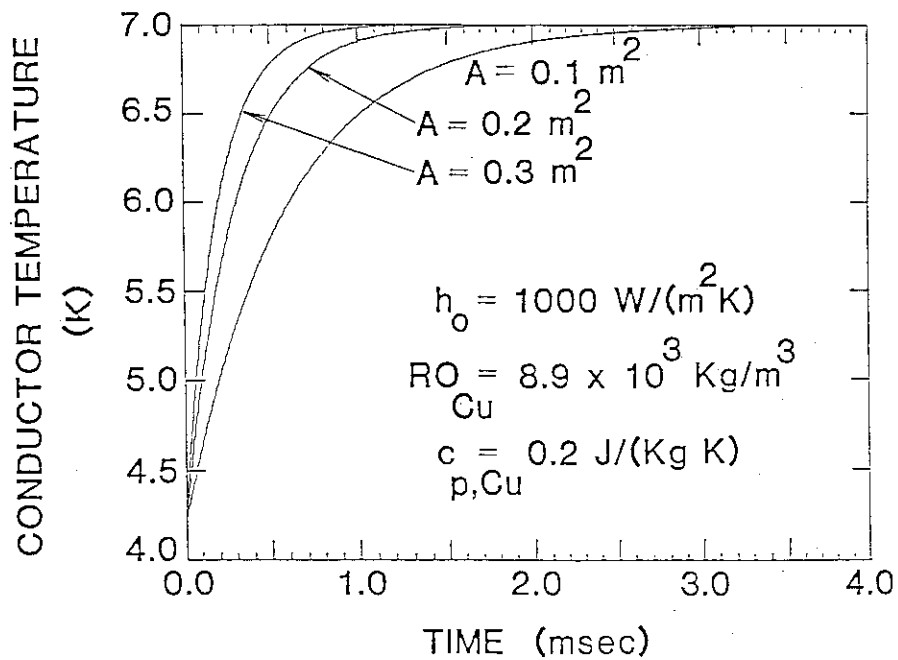


Fig. 23 Results of a "Lumped" Calculation

graph indicates that all three conductors reach the temperature of the helium by 4.0 msec and that, as expected, the conductor with the largest surface is the first to do so. Keeping in mind that the heating duration is 28 msec, it is realized that having the largest surface area offers no advantage to Coil C. The helium will remain at an elevated temperature for at least the length of the heat pulse, prohibiting any possible cooling until afterwards since 7 K is over the current sharing temperature of 5.8 K. Indeed, there is a disadvantage for Coil C in that it is the first to generate Joule heating, although a difference of one or two milliseconds is probably not enough to show up in the measured results. Thus, the nearly equivalent stability of Coil A and Coil B in vacuum is understood.

Results taken while Coil B was surrounded by helium are also displayed in Fig. 21. The stability is definitely higher. It seems likely that the presence of helium has more effect during resistive heating rather than during inductive heating--the conduit transfers heat to both the supercritical helium inside and the atmospheric pressure helium outside. The ratio of heat transferred to the outside over total heat input has not been ascertained.

Finally, a plot of the density multiplied by the specific heat, integrated from 4.2 K to the current sharing temperature, is included in Fig. 21. It is seen that there is a marked difference between it and the measured stability, some or all of which is accounted for by considering the inefficiency of the heater. Originally the remaining difference, if any, was attributed to the pressure rise during heating, as did the authors of Ref. 5, but the graph of Fig. 24 clearly indicates that the available helium heat capacity decreases with increasing pressure. The difference must therefore be the result of the introduction of fresh, cold helium to the heated zone, brought about by the induced mass flow of hot helium away from the heated zone.

The effect of the Lorentz force on the different diameter strands was also evaluated. As indicated in Fig. 25, the strands could be crowded against the outer wall of the conduit if sufficient current density and background field were provided, resulting in a loss of cooled surface area. The area loss would differ for each coil. In an extreme case the strands could actually be compacted, resulting in even more loss of surface area.

To obtain an upper bound to the displacement in the radial direction and the consequent strain in the angular direction, the simple case of a circular ring loaded by equally-spaced radial forces was considered. A formula for such a situation is provided in Ref. 15 on page 226. The two principal simplifying assumptions are 1) the angular stress due to thermal contraction is neglected (a worst-case approximation); and 2) the strands remain entirely elastic throughout the whole process. The second approximation is probably more error-prone since it has been

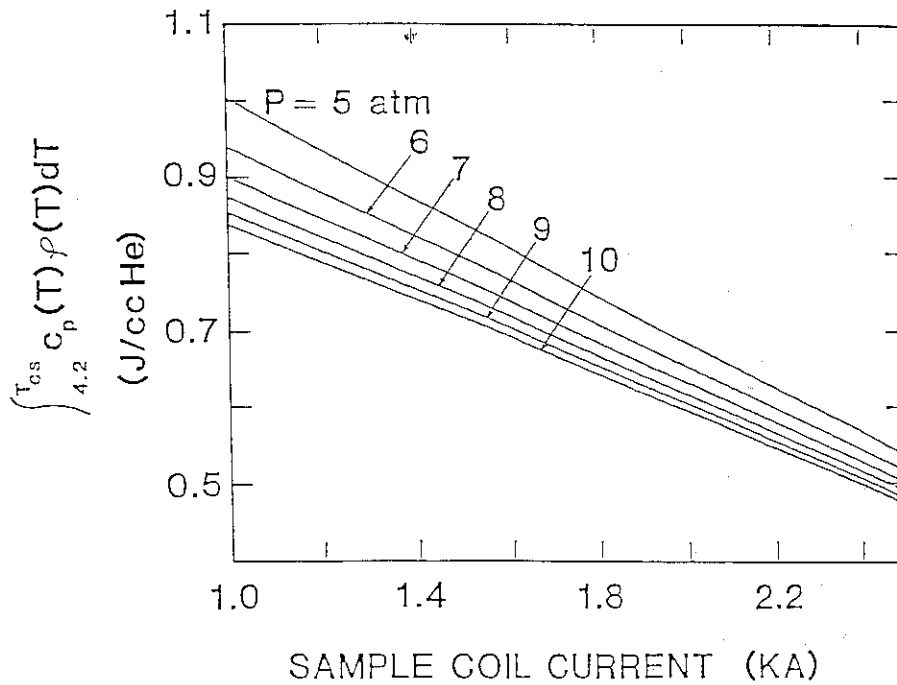


Fig. 24 Calculated Helium Heat Capacity at Various Pressures

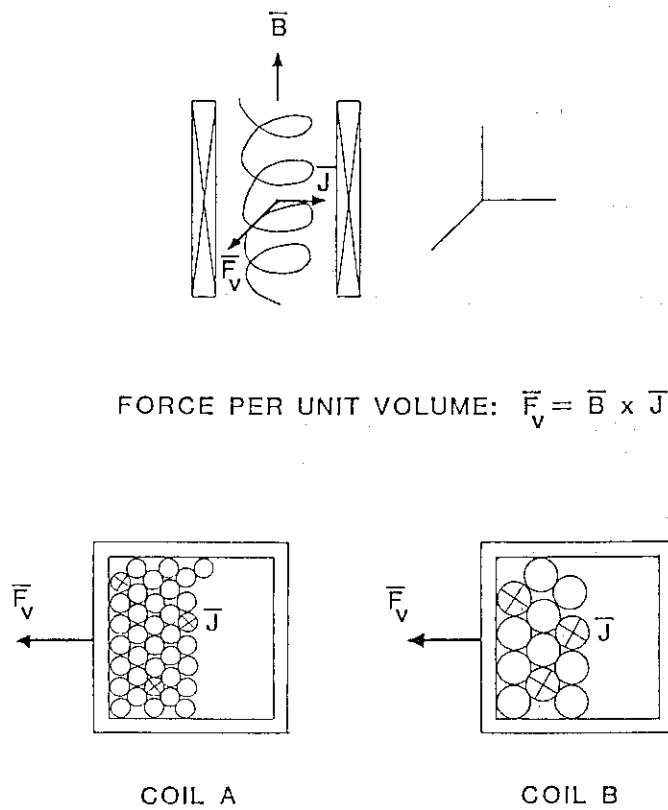


Fig. 25 Possible Lorentz Force Effects

multifilamentary conductor. [16] Thus, a more realistic model would be an inelastic ring.

A background field of 7 T and an operating current of 2.4 kA were chosen for the calculation. The load was considered to be 36 point loads spaced every 10 degrees. As anticipated, the coil with the smallest diameter strands, Coil C, suffered the largest radial displacement:  $7.5 \times 10^{-5}$  mm, corresponding to a uniaxial strain in the ring of  $7.9 \times 10^{-5}\%$ . A displacement of this magnitude is negligible, and, according to Ref. 17, this much strain should have little or no effect on the critical current of NbTi. This is especially so since the conductor is initially in a state of compression from thermal contraction. Thus, any effects from Lorentz forces are neglected.

Thermal contraction during cooldown from room temperature to 4.2 K could also affect stability. The question of whether or not the differential contraction between the conduit and the strands was briefly considered. However, since earlier work [16] reported little degradation of the critical current of Nb<sub>3</sub>Sn for conduits with void fractions equal to or greater than 50%, it is thought that the present sample coils should exhibit negligible losses in critical current, taking into account that NbTi is more ductile than Nb<sub>3</sub>Sn [17] and that the void fractions of all three coils are approximately 45%. In addition, simple reasoning concludes that the stress from thermal contraction acting on each strand is independent of strand diameter, provided that the cross-sectional area of the entire conductor is the same for the three coils. Thermal contraction is therefore also neglected with respect to a stability comparison between Coils A, B, and C.

Finally, the strand copper current density was evaluated. It was thought that the slightly different copper cross-sectional areas could result in radial heat fluxes different from what would be expected. Remembering that the strands are electrically and thermally insulated from each other, such a difference, if it occurred, could produce radically changed results. A few minutes of calculation, though, confirmed that Coil B should have the highest radial heat flux per strand, followed by Coil A and then by Coil C. It is, of course, possible that a decreased heat flux could have negative effects on stability since the induced helium flow is proportional to the heat flux. [18] That question has not been answered yet and will have to await future computer analysis.

References

1. Wilson, Martin N. Superconducting Magnets, Oxford University Press, New York, 1983.
2. Shimamoto, S., "The Japanese LCT Coil", Applied Superconductivity Conference, Baltimore, Maryland, 1986.
3. Tsuji, H., et al., "Design Selections for the Fabrication of the Demonstration Poloidal Coil", Proc. ANS 7th Topical Meeting, 1986.
4. Shimamoto, S., et al., "Evolutions in the Development of Superconducting Materials and Magnet Technology for the Coming Fusion Machines in Japan", 11th Int. Conf. on Plasma Physics and Controlled Nuclear Fusion Research, Kyoto, Japan, Nov. 1986.
5. Lue, J.W., J.R. Miller, and L. Dresner, "Stability of Cable-in-Conduit Superconductors", J. Appl. Phys. 51(1), Jan. 1980.
6. Nishi, M., et al., "A 12-T Forced Flow Type Superconducting Magnet", Applied Superconductivity Conference, Baltimore, Maryland, 1986.
7. Ohgane, Y., K. Yoshida, "Magnetic Field Calculation Code FORCE", private communication, Dept. of Thermonuclear Fusion Research, Naka Fusion Research Establishment, Japan Atomic Energy Research Institute, 1985.
8. Lue, J.W. and J.R. Miller, "Parametric Study of the Stability Margins of Cable-in-Conduit Superconductors: Experiment", IEEE Trans. Mag., MAG-17, No. 1, 1981.
9. Schmidt, C., "Stability Tests on the Euratom LCT Conductor", Cryogenics, Nov. 1984.
10. Yamaguchi, M., E. Tada, H. Saitou, and S. Shimamoto, "Stability Analysis Code ALPHE II for Forced-Cooled Superconducting Coils", JAERI-M 85-108, Dept. of Thermonuclear Fusion Research, Naka Fusion Research Establishment, Japan Atomic Energy Research Institute, 1985.
11. Tada, E., private communication.
12. Nishi, M., private communication.
13. White, Frank M., Heat Transfer, Addison-Wesley Publishing Company, U.S.A., 1984.
14. Dresner, L., "Stability of Cable-in-Conduit, Force-Cooled Conductors: Elementary Theory", ORNL/TM - 6657, 1979.
15. Roark, Raymond J. and Warren C. Young, Formulas For Stress and Strain 5th Ed., McGraw-Hill, New York, 1975.

16. Steeves, M.M. and M.O. Hoenig, "Experimental Parameter Study of Subsize Nb<sub>3</sub>Sn Cable-in-Conduit Conductors", IEEE Trans. Mag., MAG-19, No. 3, 1983.

17. Reed, Richard P. and Alan F. Clark, Materials At Low Temperatures, American Society for Metals, 1983.

18. Dresner, L., "Parametric Study of the Stability Margin of Cable-in-Conduit Superconductors: Theory", IEEE Trans. Mag., MAG-17, No. 1, 1981.

Acknowledgments

All members of the Superconducting Magnet Laboratory have greatly contributed to my well-being, both inside and outside the laboratory. I would like to single out some people who deserve special recognition:

Takahashi Yoshikazu, who was my mentor during most of my stay and who not only taught me most of what I know about superconducting magnets, but also stayed up all night on more than one occasion for my experiments;

Tsuji Hiroshi, who gave me invaluable advice and was another "all-night" experimenter;

Tada Eisuke, who was always ready and willing to discuss my problems and give me much-needed help;

Nishi Masataka, who was and is essential in the laboratory and always participated in my experiments;

Yoshida Kiyoshi, who helped me both inside and outside the laboratory;

Ando Toshinari, who gave me some of my initial instruction concerning force-cooled magnets;

Ohgane Yasuo, without whose computational advice I would have been lost;

Koizumi Kouichi and Kawano Katsumi, both of whom repeatedly came to my aid;

Matsukawa Hiroko, who knew how to do all those things that no one else knows how to do; and finally

Shimamoto Susumu, my supervisor, who made my visit here possible and to whom I owe many thanks.

Others in the S.C.M.L. include Oshikiri Masayuki, Hoshino Masahiro, Nakajima Hideo, Hiyama Tadao, and Yaguchi Eiji, all of whom I give my thanks and my best wishes.